ACS Medicinal Chemistry Letters

pubs.acs.org/acsmedchemlett

Letter

Passive Membrane Permeability of Sizable Acyclic β-Hairpin Peptides

Jillene Moxam, Sarah Naylon, Alexis D. Richaud, Guangkuan Zhao, Alberto Padilla,* and Stéphane P. Roche*

Cite This: ACS Med. Chem. Lett. 2023, 14, 278−284

Read Online

ACCESS | Metrics & More | Article Recommendations | Supporting Information

ABSTRACT: The recent shift toward increasingly larger drug modalities has created a significant demand for novel classes of compounds with high membrane permeability that can inhibit intracellular protein−protein interactions (PPIs). While major advances have been made in the design of cell-permeable helices, stapled β-sheets, and cyclic peptides, the development of large acyclic β-hairpins lags far behind. Therefore, we investigated a series of 26 β-hairpins (MW > 1.6 kDa) belonging to a chemical space *far beyond* the Lipinski "rule of five" (*fb*Ro5) and showed that, in addition to their innate plasticity, the lipophilicity of these peptides (log $D_{7.4} \approx 0 \pm 0.7$) can be tuned to drastically improve the balance between aqueous solubility and passive membrane permeability.

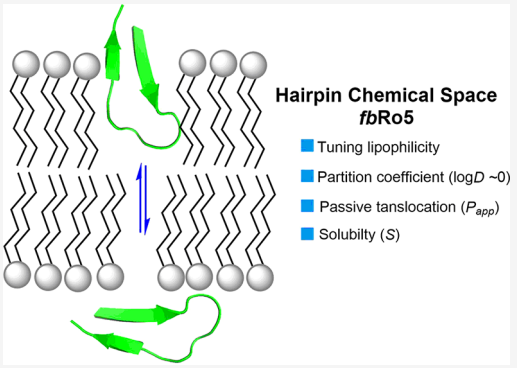

KEYWORDS: *Antibody H3 Loops, β-Hairpin Peptides, Passive Membrane Permeability, PAMPA, Beyond the Rule of 5*

In the past decade, rapid progress in genomics and proteomics led to the discovery of an unprecedented number of novel proteins engaged in protein−protein interactions (PPIs) and more complex networks.[1] Many of these PPIs are associated with disease progressions often deemed "undruggable" by our current arsenal of natural products and small-molecule drugs alike.[2] Blocking PPIs presents challenges as binding interfaces typically feature large, shallow, and potentially dynamic water-exposed surfaces, commonly not suited for small inhibitors as defined by the Lipinski's rule of five (Ro5).[3,4] Given the need for novel therapeutic modalities, larger peptides exploring a space beyond the rule of five (bRo5) are attracting a great deal of attention.[5,6] However, as rightfully questioned by Jan Kihlberg[7]—"*How big is too big for cell permeability?*"—such increase in molecular size brings on a number of challenges including rigidity, solubility, cell permeability, and ultimately oral bioavailability.[8,9] The traction by pharmas for transitioning large macrocyclic peptides in this bRo5 space to potential drug candidates spawned significant advances in understanding the major physicochemical and structural determinants responsible for artificial and cellular membrane permeation.[10−15] Recent studies on large macrocycles (MW < 1.2 kDa, 3D-PSA < 280 Å^2)[16−20] and helical peptides[21−24] have taught us that plasticity must be adjusted through intramolecular H-bonds (IMHBs) and conformational strain to reduce the molecular polar surface area (PSA) and achieve membrane permeation. In stark contrast, our current understanding of the major structural and conformational features of large acyclic β-hairpins falling *far beyond* the rule of five (*fb*Ro5: MW > 1.6 kDa; SASA > 1200 Å^2) is still at its infancy.[25−27] Our group was therefore drawn to the challenge of developing acyclic β-hairpins in this space (Figure 1) to study their properties and evaluate potential correlations between passive membrane permeability (P_{app}), lipophilicity (log $D_{7.4(ow)}$), and the hairpin tertiary structures while transitioning between aqueous-to-lipid environments. Parallel membrane permeability assays (PAMPAs) were performed to assess the impact of residual side-chain lipophilicity on permeability. As a result, we observed that, independently of the loop primary sequence, these large hairpins must retain a fine balance between lipophilicity and hydrophilicity ($|\log D_{7.4}| \leq +0.7$) to achieve a practical solubility and a relatively significant membrane permeability ($P_{app} \geq 10$ nm/s). Our circular dichroism (CD) study also demonstrated that the conformation of hairpins in water adapts into large β-structures when transitioning into a hydrophobic environment.

Given the significant role of the programmed cell death-1 protein (PD1) pairing to its ligand-1 (PDL1) as one of the major immune checkpoint exploited by cancer cells to suppress

Received: November 18, 2022
Accepted: January 24, 2023
Published: January 27, 2023

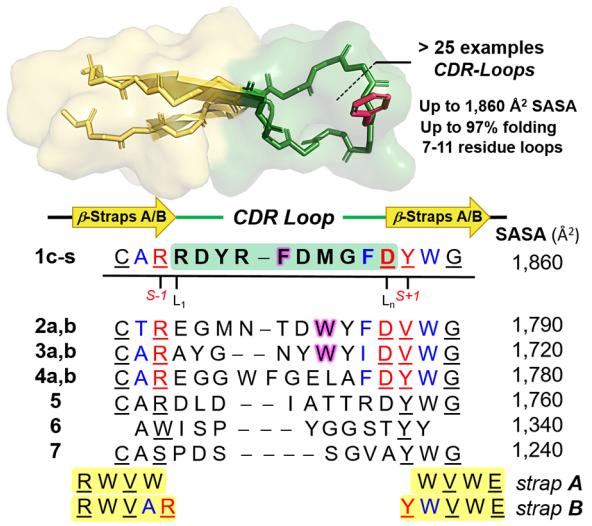

Figure 1. Primary sequence alignment of antibody CDR loops used for the library of β-hairpins (3D-model): analogs of pembrolizumab (**1c–s**), GY-14 (**2a,b**), tislelizumab (**3a,b**), durvalumab (**4a,b**), mAb59 (**5**), atezolizumab (**6**), and MW11-h317 (**7**). Regular and bulged hairpins (straps **A** and **B**) are presented in black and blue/red, respectively, with H-bonded residues underlined. Hydrophobic residues selected for substitutions by Gly are highlighted in magenta.

immune response,[28,29] our group has been interested in studying β-hairpin blockers of this particular PPI.[30,31] Recent studies have shown that cancer cells can package both PD1 and PDL1 intracellularly into exosomes, in the first scenario to be released as a decoy against anti-PD(L)1 drugs in the tumor microenvironment, and as enhancer of tumor-specific cytotoxic T-cell exhaustion in the latter scenario.[32−34] Although several anti-PD(L)1 monoclonal antibodies (mAbs) afford impressive clinical outcomes in many tumor types,[35] these drugs have disadvantages including a lack of oral bioavailability, poor tumor penetration,[36,37] and immunogenicity, leading to adverse effects.[38,39] These deficiencies underscore the need for alternative strategies including smaller molecules capable of penetrating tumor cells to target exosomal and soluble forms of PD(L)1.[40] For these reasons, we set our goal to synthesize a library of potential blockers of the PD1·PDL1 interaction by miniaturizing some of the most bioactive anti-PD(L)1 mAbs into long acyclic β-hairpins. Yet, synthetic strategies for creating β-hairpins that mimic the native loop structures found in proteins and antibodies remain largely unexplored.[41] Recently, our group reported the synthesis of β-hairpins that mimic the complementary determining region (CDR) of antibodies, and more specifically the apex of the heavy-chains 3 (CDR-H3) found in pembrolizumab.[31,42] We demonstrated that hairpins with long loops of varying plasticity can be synthesized in a highly folded state by exploiting a stabilizing β-strap motif (*str*and + *cap*)[31] that combines a tryptophan zipper motif[43] with a terminal capping originally described by Anderson.[44] Thus, we set our goal to synthesize β-hairpin mimics of mAb CDR-H3 loops, inhibitors of the PD1·PDL1 interaction, from which crystal structures have been reported. Two stabilizing motifs, straps **A** and **B** of sequences RWVW···WVWE and RWVAR···DYWVWE designed for regular and bulged hairpins, respectively, were found to be exceedingly efficient to obtain structurally folded and stable hairpins (Figure 1). In total, a library of 28 peptides encompassing seven scaffolds **1**−**7** were synthesized by solid-phase peptide synthesis (SPPS) with model peptides **1a**−**d**, 15 analogs of pembrolizumab (**1e**−**s**),[45−48] two analogs each of GY-14 (**2a,b**),[49] tislelizumab (**3a,b**),[50,51] and durvalumab (**4a,b**),[52,53] and a single analog each of mAb59 (**5**),[54] atezolizumab (**6**),[53,55] and MW11-h317 (**7**) (see Supporting Information (SI), Table S1).[56] The hairpin folds were characterized by CD spectroscopy using a typical exciton couplet at 230 ±2 nm, characteristic of the W/W cross-strand interaction in hairpin stems (see Figure 4, below).[57] Thermal denaturation experiments were performed in aqueous buffer by heating these hairpins from 0 to 95 °C, and the unfolding transitions were fitted to a two-state model equation to obtain the corresponding melting curves (see Supporting Information Excel file and Table S1).[58] As shown by the selected examples in Table 1 (*vide infra*), most hairpins **1**−**7** were relatively well-folded, and some were found to be stable to both thermal and chemical denaturation (i.e., **1f**, **1j**, **1l**, **1n**, and **3b**, χ_F > 90% at 291 K).

Analogs of CDR loops were synthesized as hairpins by SPPS and purified by semi-preparative RP-HPLC. The analytical RP-HPLC retention times of these peptides can be correlated to their overall polarity (PSA). Indeed, this series of peptides is relatively homogeneous in terms of molecular weight (MW = 1.6−2.7 kDa) and overall solvent-accessible surface area (SASA = 1200−1900 Å^2),[59] as well as the number of IMHBs within the hairpin stems, and numerous solvent-exposed amide groups (HBDs/HBAs). In this library, two hairpin scaffolds, regular-**A** and bulged-**B**, bearing a simple and positively charged polyglycine loop [$G_4K_2G_{2/4}$], were included as controls **1a,b**, along with a model of synthetic coil **1c** and the native primary sequence of pembrolizumab **1d**. As shown by their retention times on RP-HPLC (17−19 min), peptides **1a**−**c** are relatively polar, which is correlated to a largely negative partition coefficient (log $D_{7.4}$) and a poor apparent membrane permeability (P_{app} threshold of 10 nm/s).[60] The low P_{app} values measured for hairpins **1a,b** presenting a highly flexible polyglycine loop strongly suggested that the strap segments (**A** and **B**) are not inherently membrane-permeable (Figures 1 and 2). Therefore, we thought to examine a

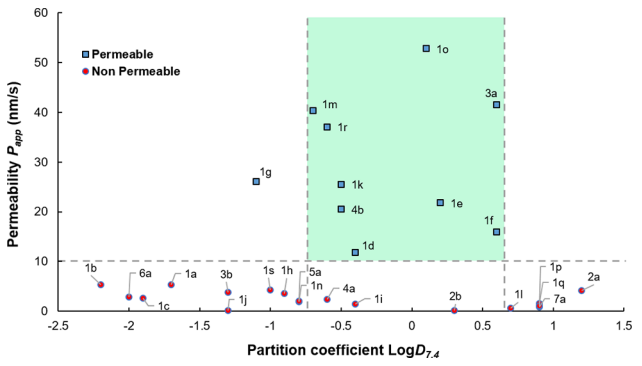

Figure 2. Passive membrane permeability (P_{app}) analysis. Dashed lines indicate the P_{app} threshold and the lipophilicity range delineating the most permeable β-hairpins within the peptide library.

potential correlation between P_{app} and lipophilicity among the different hairpin loops to determine if the log $D_{7.4}$ values could be used as a predictor of membrane permeation.

During the initial screening, 28 peptides were evaluated by PAMPA in 96-well plates, and the P_{app} value averages of triplicate experiments were obtained for each compound (SI,

https://doi.org/10.1021/acsmedchemlett.2c00486
ACS Med. Chem. Lett. 2023, 14, 278−284

Figure S4). The artificial membranes' integrity was established for each plate with Lucifer yellow as negative control (P_{app} = 5.4 ± 0.6 nm/s) and with warfarin (P_{app} = 70.6 ± 5.4 nm/s), a known cell-permeable drug to ensure PAMPA reproducibility and to detect compounds having a high passive membrane diffusion.[61,62] Overall, the coefficients of variation of P_{app} obtained between all PAMPA plates (CV ≤ 11%) are indicatative of a strong reproducibility between experiments. Across the different folded hairpins **1**–**7**, a strong inverse correlation between kinetic aqueous solubility (S) and log $D_{7.4}$ was observed (see Table 1). Indeed, we found that large

Table 1. Selected Examples of Lipophilicity Scanning from Varying Loops and Hairpin Scaffolds (Physicochemical Properties at 291 K)

ID	%-fold[a]	T_R [b]	S [c]	log$D_{7.4}$[d]	P_{app}[e]
1c	*RC*	18.8	18.0	-1.9 ± 0.4	2.6 ± 1.8
1e	50 ± 1%	23.1	0.01	0.2 ± 0.1	**21.8 ± 12.3***
1f	92 ± 1%	21.5	0.02	0.6 ± 0.2	**15.9 ± 6.0***
1g	49 ± 2%	23.0	0.02	-1.1 ± 0.8	**26.1 ± 7.4***
1h	89 ± 1%	20.6	0.03	-0.9 ± 0.5	0.4 ± 0.9
1i	37 ± 1%	21.9	0.02	-0.4 ± 0.3	1.4 ± 2.3
1j	92 ± 1%	19.5	1.80	-1.3 ± 0.3	0.2 ± 0.2
1k	48 ± 1%	21.8	0.01	**-0.5 ± 0.4**	**25.5 ± 23.4***
1l	97 ± 1%	20.3	0.04	0.7 ± 0.5	0.7 ± 0.5
1m	50 ± 1%	22.6	**0.05**	**0.7 ± 0.4**	**40.4 ± 26.2***
1n	97 ± 1%	20.9	0.06	-0.8 ±0.4	0.2 ± 0.6
1o	40 ± 1%	25.2	0.02	**0.1 ± 0.4**	**52.8 ± 45.0***
1p	81 ± 1%	23.3	0.02	0.9 ± 0.4	0.1 ± 0.2
1r	*cyclic*	22.0	0.01	-0.6 ± 0.1	**37.1 ± 16.3***
2a	36 ± 2%	23.3	0.02	1.2 ± 0.4	4.2 ± 2.6
2b	36 ± 1%	21.1	0.69	0.3 ± 0.6	0.2 ± 0.1
3a	β-sheet	24.1	0.002	0.6 ± 0.1	**41.5 ± 18.7***
3b	91 ± 1%	21.9	0.07	-1.3 ± 0.3	3.8 ± 6.9
4b	β-sheet	21.2	**0.26**	**-0.5± 0.1**	**20.5 ± 4.3**
5a	78 ± 1%	23.2	0.14	0.8 ± 0.6	2.0 ± 1.1
7a	85 ± 1%	22.8	0.53	0.9 ± 0.6	0.9 ± 0.3

[a]Hairpin folded fractions at 291 K calculated from the best-fitted melting curves of thermal denaturation recorded by CD spectroscopy. [b]Retention times (min) determined by analytical RP-HPLC. [c]Kinetic solubility (mM) measured in a phosphate buffer (PB, 50 mM) at pH 7.4 (N = 3). [d]Partition coefficients (octanol–PB) measured by shake flask assay and reported as mean values ± s.d. (N = 3). [e]Apparent membrane permeability values (nm/s) determined by PAMPA (pH of 7.4) at 291 K. Data reported as the mean of three (N = 3) or nine replicates (N = 9, marked with a star) with s.d. calculated across those experiments.

octanol–water partition coefficients for either highly lipophilic or hydrophilic compounds |log $D_{7.4}$| > 0.7 correlated strongly with peptides having the weakest membrane permeability. Our results on this particular set of hairpins suggested that peptides able to cross this artificial membrane model had typically log $D_{7.4}$ values close to zero (−0.26 ± 0.54, mean ± s.d. with N = 9). As shown in Figure 2, peptides that were not permeable have a higher average and a wider dispersion of log $D_{7.4}$ values. Even if the log $D_{7.4}$ appeared as a relatively accurate predictor of membrane permeation, satisfying the rule of |log $D_{7.4}$| ≤ + 0.7 did not consistently afford permeable peptides (blue markers, Figure 2). These results support the idea that a balance between polarity, lipophilicity, and solubility might be required in order to yield a measurable passive permeability for these remarkably large hairpin peptides (MW = 1.6–2.5 kDa).[63]

We previously demonstrated that replacing the Phe residue within the loop of hairpins **1e** and **1o** by Gly resulted in enhancing both the solubility and the %-folding of analogs **1f** and **1p**.[31] In turn, this modification enabled the full structural NMR characterization of these β-hairpins. Although hairpins **1f**/**1p** were about 40% more folded than **1e**/**1o**, their retention times measured by RP-HPLC were shorter (~2 min), suggesting that the Gly analogs were inherently more polar (Table 1). To further establish a possible trend between passive permeation and lipophilicity, we therefore evaluated seven congeneric pairs of hairpin loops based on a single side-chain modulation, Phe/Trp → Gly (see positions in Figure 1, and results in Figure 3). As shown by their retention times of

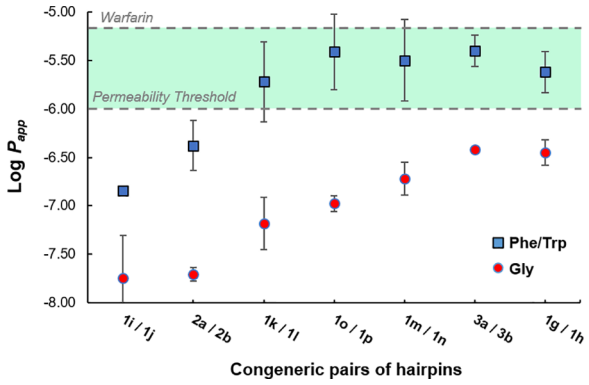

Figure 3. Correlation plot between passive permeation and lipophilicity by single side-chain modulation within the hairpin loops. Original loops with Phe/Trp and their Gly-derived analogs.

22–24 min in Table 1, the original yet less folded hairpin mimics of pembrolizumab (**1e**, **1g**, **1i**, **1k**, **1m**), GY-14 (**2a**), and tislelizumab (**3a**) were strikingly more hydrophobic than their Gly analogs (**1f**, **1h**, **1j**, **1l**, **1n**, **2b**, and **3b**, T_R = 20–22 min). In addition, normalized HPLC retention times showed a relatively strong correlation to our experimental log $D_{7.4}$ across the library (SI, Figure S3). These results further confirm that the global %-folding of such large hairpins (and potentially the overall number of IMHBs) is not a major contributor to the net physicochemical properties of these molecules. As shown in Figure 3, the F10G substitution in the loops of each pembrolizumab analog (**1e**–**n**), but also the W12G in the loop of **2a** vs **2b**, and the W11G substitution in the loop of **3a** vs **3b**, had in each case a similar detrimental effect on passive membrane permeability. Across the entire set of congeneric pairs, we measured a 10- to 50-fold reduction in P_{app} on average between the original most hydrophobic hairpins and their glycine-derived analogs. Although hairpins with a Gly-mutated loop adopt a more stable fold (higher %-folding and thermal stability T_m), the drop of lipophilicity imparted by the removal of a single hydrophobic residue (e.g., Phe and Trp) reduced their permeability properties. In addition, hairpins wrapped around a bulge strap **B**, such as **1e**, achieved high membrane permeability with either a V18H substitution in the strap of **1k** or a D15N replacement within the bulge of **1m**

https://doi.org/10.1021/acsmedchemlett.2c00486
ACS Med. Chem. Lett. 2023, 14, 278–284

(Table 1). Yet, adding a charged residue (His or Lys) within the strap of hairpins **1i**–**l** did not improve their passive permeation in comparison to the more lipophilic analogs **1e**–**h**. Finally, a macrocyclic hairpin **1r** (analog of **1e**), stapled through a disulfide linkage, was also tested and revealed a 2-fold increase in membrane permeability. As shown in Table 1, a total nine peptides—eight acyclic hairpins **1e**–**g**, **1k**, **1m**, **1o**, **3a**, and **4b** with a significantly high passive permeability comparable to that of the macrocycle **1r**—were identified from the library despite their large size. For most of these compounds, P_{app} values were confirmed on three separate PAMPA plates and on different days. Taken together, the two peptides **1m** and **4b** appeared to possess the most promising balanced properties between solubility, log $D_{7.4}$, and membrane permeability. We concluded that hydrophobic residues at the apex of hairpin loops are likely more exposed to water, which significantly enhances molecular lipophilicity and enables sizable hairpins to passively translocate through membranes.

It is becoming increasingly evident that even strained macrocyclic peptides should retain some backbone flexibility to "actively" penetrate and translocate through membranes.[10,18−20] Indeed, this effect of plasticity on the conformational behavior of peptides between aqueous and lipophilic media is an important area of investigation to inform the design of cell-permeable (macro)molecules. In fact, the enthalpy−entropy compensation required of peptides and other drug-like small molecules during membrane translocation entails a number of events within the solute−water and solute−lipid interactions. For example, the folding of polar groups (via IMHBs) has been shown to decrease the overall PSA of flexible molecules and lower the energetic cost of desolvation associated with passive cell penetration, often resulting in increasing molecular compactness during translocation.[64,65] As eluded by Fouché in a recent study of large macrocyclic peptides (decamers, MW ≈ 1.0 kDa),[66] a high structural rigidity in the apolar membrane environment might not be beneficial, whereas a flexible backbone would afford an entropic benefit and a driving force to more actively diffuse. Several other groups drew a similar conclusion that large molecules (MW ≥ 1.0 kDa) are more likely to achieve membrane permeation if they possess an important conformational chameleonicity. To test this notion of conformational flexibility, four of the most membrane permeable hairpins (**1g**, **1k**, **1m**, and **1o**) were selected, and their far-UV CD spectra were recorded in aqueous media (pH 7.4) and in a membrane-like media of octanol (Figure 4).[67−69] The small amounts of methanol cosolvent (20% v/v) added to both aqueous and octanol peptide solutions for consistency were shown to enhance solubility without affecting the hairpin folds and the overall CD spectra (see Figure S2).

As expected, the tertiary structure of these hairpins in phosphate buffer was characterized by an intense $\pi-\pi^*$ exciton couplet maximum at 230 ± 2 nm of the Trp/Trp pair interactions (indole T-shape stacking), and in most cases by a positive band at 204 ± 1 nm, likely generated by the kinked β-bulge within strap **B** (Figure 4A).[57] Strikingly, in octanol, a complete shift of the main band wavelength at 230 nm to β-sheet band at 215 ± 1 nm was observed with an overall larger intensity in molar ellipticity (Figure 4B). This drastic change of three-dimensional structure clearly indicates that the hairpin folds are largely disrupted in octanol[70] by forming extended intra- or intermolecular β-structures.[71] Given the order of magnitude of the new β-sheet band at 215 nm (θ of 170,000° to 340,000°) a supramolecular assembly of β-hairpins might take place in a more lipophilic environment.[72] These results indicate that the four acyclic hairpin considered are highly flexible, which would be consistent with a minimization of entropic cost through conformational rearrangement in a membrane-like environment. While hairpins **1g**/**1k** remained largely folded (exciton intensity at 230 nm) in octanol, the two most membrane permeable hairpins **1m**/**1o** (see Table 1) were completely converted into a different β-structure (no observable 230 nm exciton). Collectively, these results complement the octanol−water model to suggest that the lipophilicity and the conformational flexibility of these long acyclic hairpins are two key determinants of passive membrane permeation.

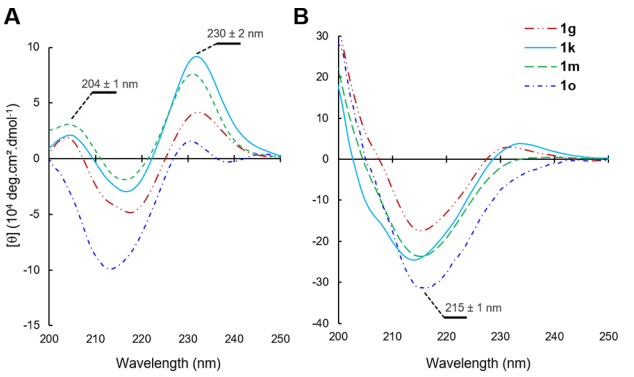

Figure 4. CD spectra comparison of peptides **1g**, **1k**, **1m**, and **1o** (**A**) in a 50 mM phosphate buffer (pH 7.4), and (**B**) in octanol with addition of MeOH (1:4 v/v) in each case.

In conclusion, we demonstrated that out of a library of 28 peptides, nine hairpins have significant passive membrane permeability (from only three different loop sequences). Overall, the PAMPA results showed a significant correlation between membrane permeability and lipophilicity ($|\log D_{7.4}| \leq +0.7$). In each case, replacing Gly by Phe/Trp residues within the loops resulted in hairpins with high passive permeability. Our results also revealed that these hairpins are innately flexible and can adapt into different β-structures in a lipophilic environment. This suggests that hairpins may alter their tertiary structure during membrane translocation. Although the size and polarity of the β-hairpins evaluated herein generally fail to meet the common criteria of drug-likeness, our study demonstrated that such chemotypes (*fb*Bro5: MW = 1.6−2.5 kDa, loop SASA > 500 Å^2) can exhibit passive permeability similar to that of small molecules. This study is important in showing that some antibody CDR loops can be incorporated into large yet permeable β-hairpin scaffolds.[73] Further NMR and computational studies of the hairpin backbone rigidity and the change of tertiary structures will be required to understand the potential of this largely untapped chemical space. We hope that our results will inform and stimulate future studies on β-hairpins and other large proteomimetic scaffolds that will extend a chemical space *fb*Ro5 toward bioactive molecules offering uniquely large three-dimensional surface areas for protein binding.

■ ASSOCIATED CONTENT

Supporting Information

The Supporting Information is available free of charge at https://pubs.acs.org/doi/10.1021/acsmedchemlett.2c00486.

https://doi.org/10.1021/acsmedchemlett.2c00486
ACS Med. Chem. Lett. 2023, 14, 278−284

Supplementary data summarizing the synthetic protocols for all the peptides, their purity, structural characterization by CD spectroscopy, and the PAMPA results (PDF)

CD data (XLSX)

AUTHOR INFORMATION

Corresponding Authors

Stéphane P. Roche − *Department of Chemistry and Biochemistry, Florida Atlantic University, Boca Raton, Florida 33431, United States; Center for Molecular Biology and Biotechnology, Florida Atlantic University, Jupiter, Florida 33458, United States;* orcid.org/0000-0002-3019-2168; Email: sroche2@fau.edu

Alberto Padilla − *Department of Natural Science, Keiser University, Fort Lauderdale, Florida 33309, United States;* Email: apadilla@keiseruniversity.edu

Authors

Jillene Moxam − *Department of Chemistry and Biochemistry, Florida Atlantic University, Boca Raton, Florida 33431, United States*

Sarah Naylon − *Department of Chemistry and Biochemistry, Florida Atlantic University, Boca Raton, Florida 33431, United States*

Alexis D. Richaud − *Department of Chemistry and Biochemistry, Florida Atlantic University, Boca Raton, Florida 33431, United States*

Guangkuan Zhao − *Department of Chemistry and Biochemistry, Florida Atlantic University, Boca Raton, Florida 33431, United States*

Complete contact information is available at: https://pubs.acs.org/10.1021/acsmedchemlett.2c00486

Author Contributions

This project was conceived by A.P. and S.P.R. Peptide syntheses, purifications, analyses, and thermal denaturations were achieved by S.N., A.D.R., and G.Z. CD analyses in various media were obtained and treated by A.D.R., and PAMPA experiments were carried out by J.M. S.P.R. wrote the manuscript with the contribution of A.P. and A.D.R. All authors have given approval to the final version of the manuscript.

Notes

The authors declare no competing financial interest.

ACKNOWLEDGMENTS

We are very grateful for the financial support from the U.S. National Institutes of Health (NIGMS Grant R21GM132754 to A.D.R., G.Z., and S.P.R.). The authors also thank Mr. Adrian Romoff from Florida Atlantic University for the preliminary data on hairpin folding by CD spectroscopy.

ABBREVIATIONS

bRo5, beyond the rule of five; CDR, complementary determining region; MW, molecular weight; PSA, polar surface area; SASA, solvent-accessible surface area; HBDs/HBAs, hydrogen bond donors and acceptors; HPLC, high-pressure liquid chromatography; NMR, nuclear magnetic resonance; CD, circular dichroism

REFERENCES

(1) Legrain, P.; Rain, J.-C. Twenty years of protein interaction studies for biological function deciphering. *J. Proteomics* **2014**, *107*, 93.

(2) Scott, D. E.; Bayly, A. R.; Abell, C.; Skidmore, J. Small molecules, big targets: drug discovery faces the protein-protein interaction challenge. *Nat. Rev. Drug Discovery* **2016**, *15*, 533.

(3) Ran, X.; Gestwicki, J. E. Inhibitors of protein-protein interactions (PPIs): an analysis of scaffold choices and buried surface area. *Curr. Opin. Chem. Biol.* **2018**, *44*, 75.

(4) Shultz, M. D. Two Decades under the Influence of the Rule of Five and the Changing Properties of Approved Oral Drugs. *J. Med. Chem.* **2019**, *62*, 1701.

(5) Qian, Z.; Dougherty, P. G.; Pei, D. Targeting intracellular protein-protein interactions with cell-permeable cyclic peptides. *Curr. Opin. Chem. Biol.* **2017**, *38*, 80.

(6) Peraro, L.; Kritzer, J. A. Emerging Methods and Design Principles for Cell-Penetrant Peptides. *Angew. Chem., Int. Ed.* **2018**, *57*, 11868.

(7) Matsson, P.; Kihlberg, J. How Big Is Too Big for Cell Permeability? *J. Med. Chem.* **2017**, *60*, 1662.

(8) Wang, H.; Dawber, R. S.; Zhang, P.; Walko, M.; Wilson, A. J.; Wang, X. Peptide-based inhibitors of protein-protein interactions: biophysical, structural and cellular consequences of introducing a constraint. *Chem. Sci.* **2021**, *12*, 5977.

(9) Doak, B. C. C.; Over, B. B.; Giordanetto, F.; Kihlberg, J. Oral Druggable Space beyond the Rule of 5: Insights from Drugs and Clinical Candidates. *Chem. Biol.* **2014**, *21*, 1115.

(10) Over, B.; Matsson, P.; Tyrchan, C.; Artursson, P.; Doak, B. C; Foley, M. A; Hilgendorf, C.; Johnston, S. E; Lee, M. D; Lewis, R. J; McCarren, P.; Muncipinto, G.; Norinder, U.; Perry, M. W D; Duvall, J. R; Kihlberg, J. Structural and conformational determinants of macrocycle cell permeability. *Nat. Chem. Biol.* **2016**, *12*, 1065.

(11) Naylor, M. R.; Bockus, A. T.; Blanco, M.-J.; Lokey, R. S. Cyclic peptide natural products chart the frontier of oral bioavailability in the pursuit of undruggable targets. *Curr. Opin. Chem. Biol.* **2017**, *38*, 141.

(12) Walport, L. J.; Obexer, R.; Suga, H. Strategies for transitioning macrocyclic peptides to cell-permeable drug leads. *Curr. Opin. Biotechnol.* **2017**, *48*, 242.

(13) Vinogradov, A. A.; Yin, Y.; Suga, H. Macrocyclic Peptides as Drug Candidates: Recent Progress and Remaining Challenges. *J. Am. Chem. Soc.* **2019**, *141*, 4167.

(14) Appiah Kubi, G.; Dougherty, P. G.; Pei, D. Designing Cell-Permeable Macrocyclic Peptides. In *Cyclic Peptide Design*; Goetz, G., Ed.; Springer: New York, 2019; pp 41−59.

(15) Caron, G.; Kihlberg, J.; Goetz, G.; Ratkova, E.; Poongavanam, V.; Ermondi, G. Steering New Drug Discovery Campaigns: Permeability, Solubility, and Physicochemical Properties in the bRo5 Chemical Space. *ACS Med. Chem. Lett.* **2021**, *12*, 13.

(16) Rezai, T.; Bock, J. E.; Zhou, M. V.; Kalyanaraman, C.; Lokey, R. S.; Jacobson, M. P. Conformational Flexibility, Internal Hydrogen Bonding, and Passive Membrane Permeability: Successful in Silico Prediction of the Relative Permeabilities of Cyclic Peptides. *J. Am. Chem. Soc.* **2006**, *128*, 14073.

(17) Whitty, A.; Zhong, M.; Viarengo, L.; Beglov, D.; Hall, D. R.; Vajda, S. Quantifying the chameleonic properties of macrocycles and other high-molecular-weight drugs. *Drug Discovery Today* **2016**, *21*, 712.

(18) Tyagi, M.; Poongavanam, V.; Lindhagen, M.; Pettersen, A.; Sjö, P.; Schiesser, S.; Kihlberg, J. Toward the Design of Molecular Chameleons: Flexible Shielding of an Amide Bond Enhances Macrocycle Cell Permeability. *Org. Lett.* **2018**, *20*, 5737.

(19) Le Roux, A.; Blaise, É.; Boudreault, P.-L.; Comeau, C.; Doucet, A.; Giarrusso, M.; Collin, M.-P.; Neubauer, T.; Kölling, F.; Göller, A. H.; Seep, L.; Tshitenge, D. T.; Wittwer, M.; Kullmann, M.; Hillisch, A.; Mittendorf, J.; Marsault, E. Structure-Permeability Relationship of Semipeptidic Macrocycles-Understanding and Optimizing Passive Permeability and Efflux Ratio. *J. Med. Chem.* **2020**, *63*, 6774.

(20) Sheikh, A. Y.; Mattei, A.; Miglani Bhardwaj, R.; Hong, R. S.; Abraham, N. S.; Schneider-Rauber, G.; Engstrom, K. M.; Diwan, M.; Henry, R. F.; Gao, Y.; Juarez, V.; Jordan, E.; DeGoey, D. A.; Hutchins, C. W. Implications of the Conformationally Flexible, Macrocyclic Structure of the First-Generation, Direct-Acting Anti-Viral Paritaprevir on Its Solid Form Complexity and Chameleonic Behavior. *J. Am. Chem. Soc.* **2021**, *143*, 17479.
(21) Muppidi, A.; Doi, K.; Edwardraja, S.; Drake, E. J.; Gulick, A. M.; Wang, H.-G.; Lin, Q. Rational Design of Proteolytically Stable, Cell-Permeable Peptide-Based Selective Mcl-1 Inhibitors. *J. Am. Chem. Soc.* **2012**, *134*, 14734.
(22) Yamashita, H.; Demizu, Y.; Shoda, T.; Sato, Y.; Oba, M.; Tanaka, M.; Kurihara, M. Amphipathic short helix-stabilized peptides with cell-membrane penetrating ability. *Bioorg. Med. Chem.* **2014**, *22*, 2403.
(23) Bird, G. H.; Mazzola, E.; Opoku-Nsiah, K.; Lammert, M. A.; Godes, M.; Neuberg, D. S.; Walensky, L. D. Biophysical determinants for cellular uptake of hydrocarbon-stapled peptide helices. *Nat. Chem. Biol.* **2016**, *12*, 845.
(24) Tian, Y.; Jiang, Y.; Li, J.; Wang, D.; Zhao, H.; Li, Z. Effect of Stapling Architecture on Physiochemical Properties and Cell Permeability of Stapled α-Helical Peptides: A Comparative Study. *ChemBioChem.* **2017**, *18*, 2087.
(25) Sinthuvanich, C.; Veiga, A. S.; Gupta, K.; Gaspar, D.; Blumenthal, R.; Schneider, J. P. Anticancer β-Hairpin Peptides: Membrane-Induced Folding Triggers Activity. *J. Am. Chem. Soc.* **2012**, *134*, 6210.
(26) Gupta, K.; Jang, H.; Harlen, K.; Puri, A.; Nussinov, R.; Schneider, J. P.; Blumenthal, R. Mechanism of Membrane Permeation Induced by Synthetic β-Hairpin Peptides. *Biophys. J.* **2013**, *105*, 2093−2103.
(27) Miller, S. E.; Schneider, J. P. The effect of turn residues on the folding and cell-penetrating activity of β-hairpin peptides and applications toward protein delivery. *Pept. Sci.* **2020**, *112*, No. e24125.
(28) Boussiotis, V. A. Molecular and Biochemical Aspects of the PD-1 Checkpoint Pathway. *N. Engl. J. Med.* **2016**, *375*, 1767.
(29) De Sousa Linhares, A.; Leitner, J.; Grabmeier-Pfistershammer, K.; Steinberger, P. Not All Immune Checkpoints Are Created Equal. *Front. Immunol.* **2018**, *9*, 1909.
(30) Lepir, T.; Zaghouani, M.; Roche, S. P.; Li, Y. Y.; Suarez, M.; Irias, M. J.; Savaraj, N. Nivolumab to pembrolizumab switch induced a durable melanoma response: A case report. *Medicine* **2019**, *98*, No. e13804.
(31) Richaud, A. D.; Zaghouani, M.; Zhao, G.; Wangpaichitr, M.; Savaraj, N.; Roche, S. P. Exploiting the Innate Plasticity of the Programmed Cell Death-1 (PD1) Receptor to Design Pembrolizumab H3 Loop Mimics. *ChemBioChem* **2022**, *23*, No. e202200449.
(32) Yang, Y.; Li, C.-W.; Chan, L.-C.; Wei, Y.; Hsu, J.-M.; Xia, W.; Cha, J.-H.; Hou, J.; Hsu, J. L.; Sun, L.; Hung, M.-C. Exosomal PD-L1 harbors active defense function to suppress T cell killing of breast cancer cells and promote tumor growth. *Cell Res.* **2018**, *28*, 862.
(33) Chen, G.; Huang, A. C.; Zhang, W.; Zhang, G.; Wu, M.; Xu, W.; Yu, Z.; Yang, J.; Wang, B.; Sun, H.; Xia, H.; Man, Q.; Zhong, W.; Antelo, L. F.; Wu, B.; Xiong, X.; Liu, X.; Guan, L.; Li, T.; Liu, S.; Yang, R.; Lu, Y.; Dong, L.; McGettigan, S.; Somasundaram, R.; Radhakrishnan, R.; Mills, G.; Lu, Y.; Kim, J.; Chen, Y. H.; Dong, H.; Zhao, Y.; Karakousis, G. C.; Mitchell, T. C.; Schuchter, L. M.; Herlyn, M.; Wherry, E. J.; Xu, X.; Guo, W. Exosomal PD-L1 contributes to immunosuppression and is associated with anti-PD-1 response. *Nature* **2018**, *560*, 382.
(34) Poggio, M.; Hu, T.; Pai, C.-C.; Chu, B.; Belair, C. D.; Chang, A.; Montabana, E.; Lang, U. E.; Fu, Q.; Fong, L.; Blelloch, R. Suppression of Exosomal PD-L1 Induces Systemic Anti-tumor Immunity and Memory. *Cell* **2019**, *177*, 414.
(35) Sharma, P.; Allison, J. P. Immune Checkpoint Targeting in Cancer Therapy: Toward Combination Strategies with Curative Potential. *Cell* **2015**, *161*, 205.
(36) Thurber, G. M.; Schmidt, M. M.; Wittrup, K. D. Antibody tumor penetration: Transport opposed by systemic and antigen-mediated clearance. *Adv. Drug Delivery Rev.* **2008**, *60*, 1421.
(37) Vasalou, C.; Helmlinger, G.; Gomes, B. A Mechanistic Tumor Penetration Model to Guide Antibody Drug Conjugate Design. *PLoS One* **2015**, *10*, No. e0118977.
(38) Wang, Y.; Zhou, S.; Yang, F.; Qi, X.; Wang, X.; Guan, X.; Shen, C.; Duma, N.; Vera Aguilera, J.; Chintakuntlawar, A.; Price, K. A.; Molina, J. R.; Pagliaro, L. C.; Halfdanarson, T. R.; Grothey, A.; Markovic, S. N.; Nowakowski, G. S.; Ansell, S. M.; Wang, M. L. Treatment-Related Adverse Events of PD-1 and PD-L1 Inhibitors in Clinical Trials: A Systematic Review and Meta-analysis. *JAMA Oncol.* **2019**, *5*, 1008.
(39) Delanoy, N.; Champiat, S.; Massard, C.; Ribrag, V.; Marabelle, A.; Michot, J.-M.; Comont, T.; Dupont, R.; Kramkimel, N.; Lazarovici, J.; Chahine, C.; Madonna, E.; Robert, C.; Besse, B.; Mateus, C.; Pautier, P.; Albiges, L.; Herbaux, C.; Guillemin, A.; Saiag, P.; Maerevoet, M.; Bout, J.-C.; Leduc, C.; Biscay, P.; Quere, G.; Nardin, C.; Ebbo, M.; Marret, G.; Levrat, V.; Dujon, C.; Vargaftig, J.; Laghouati, S.; Voisin, A.-L.; Croisille, L.; Godeau, B.; Michel, M.; Lambotte, O. Haematological immune-related adverse events induced by anti-PD-1 or anti-PD-L1 immunotherapy: a descriptive observational study. *Lancet Haematol.* **2019**, *6*, No. e48.
(40) Nowicki, T. S.; Hu-Lieskovan, S.; Ribas, A. Mechanisms of Resistance to PD-1 and PD-L1 Blockade. *Cancer J.* **2018**, *24*, 47.
(41) Mullard, A. Protein-protein interaction inhibitors get into the groove. *Nat. Rev. Drug Discovery* **2012**, *11*, 173−175. Rognan, D. Rational design of protein-protein interaction inhibitors. *MedChemComm* **2015**, *6*, 51.
(42) Richaud, A. D.; Zhao, G.; Hobloss, S.; Roche, S. P. Folding in Place: Design of β-Strap Motifs to Stabilize the Folding of Hairpins with Long Loops. *J. Org. Chem.* **2021**, *86*, 13535.
(43) Cochran, A. G.; Skelton, N. J.; Starovasnik, M. A. Tryptophan zippers: Stable, monomeric $\boldsymbol{\beta}$-hairpins. *Proc. Natl. Acad. Sci. U.S.A.* **2001**, *98*, 5578.
(44) Anderson, J. M.; Kier, B. L.; Shcherbakov, A. A.; Andersen, N. H. An improved capping unit for stabilizing the ends of associated β-strands. *FEBS Lett.* **2014**, *588*, 4749.
(45) Scapin, G.; Yang, X.; Prosise, W. W.; McCoy, M.; Reichert, P.; Johnston, J. M.; Kashi, R. S.; Strickland, C. Structure of full-length human anti-PD1 therapeutic IgG4 antibody pembrolizumab. *Nat. Struct. Mol. Biol.* **2015**, *22*, 953.
(46) Lee, J. Y.; Lee, H. T.; Shin, W.; Chae, J.; Choi, J.; Kim, S. H.; Lim, H.; Won Heo, T.; Park, K. Y.; Lee, Y. J.; Ryu, S. E.; Son, J. Y.; Lee, J. U.; Heo, Y.-S. Structural basis of checkpoint blockade by monoclonal antibodies in cancer immunotherapy. *Nat. Commun.* **2016**, *7*, 13354.
(47) Horita, S.; Nomura, Y.; Sato, Y.; Shimamura, T.; Iwata, S.; Nomura, N. High-resolution crystal structure of the therapeutic antibody pembrolizumab bound to the human PD-1. *Sci. Rep.* **2016**, *6*, 35297.
(48) Na, Z.; Yeo, S. P.; Bharath, S. R.; Bowler, M. W.; Balıkçı, E.; Wang, C.-I.; Song, H. Structural basis for blocking PD-1-mediated immune suppression by therapeutic antibody pembrolizumab. *Cell Res.* **2017**, *27*, 147.
(49) Chen, D.; Tan, S.; Zhang, H.; Wang, H.; He, W.; Shi, R.; Tong, Z.; Zhu, J.; Cheng, H.; Gao, S.; Chai, Y.; Qi, J.; Xiao, M.; Yan, J.; Gao, G. F. The FG Loop of PD-1 Serves as a "Hotspot" for Therapeutic Monoclonal Antibodies in Tumor Immune Checkpoint Therapy. *iScience* **2019**, *14*, 113.
(50) Lee, S. H.; Lee, H. T.; Lim, H.; Kim, Y.; Park, U. B.; Heo, Y.-S. Crystal structure of PD-1 in complex with an antibody-drug tislelizumab used in tumor immune checkpoint therapy. *Biochem. Biophys. Res. Commun.* **2020**, *527*, 226.
(51) Hong, Y.; Feng, Y.; Sun, H.; Zhang, B.; Wu, H.; Zhu, Q.; Li, Y.; Zhang, T.; Zhang, Y.; Cui, X.; Li, Z.; Song, X.; Li, K.; Liu, M.; Liu, Y. Tislelizumab uniquely binds to the CC′ loop of PD-1 with slow-dissociated rate and complete PD-L1 blockage. *FEBS Open Bio.* **2021**, *11*, 782.

https://doi.org/10.1021/acsmedchemlett.2c00486
ACS Med. Chem. Lett. 2023, 14, 278−284

(52) Tan, S.; Liu, K.; Chai, Y.; Zhang, C. W. H.; Gao, S.; Gao, G. F.; Qi, J. Distinct PD-L1 binding characteristics of therapeutic monoclonal antibody durvalumab. *Protein Cell* **2018**, *9*, 135.
(53) Lee, H. T.; Lee, J. Y.; Lim, H.; Lee, S. H.; Moon, Y. J.; Pyo, H. J.; Ryu, S. E.; Shin, W.; Heo, Y.-S. Molecular mechanism of PD-1/PD-L1 blockade via anti-PD-L1 antibodies atezolizumab and durvalumab. *Sci. Rep.* **2017**, *7*, 5532.
(54) Liu, J.; Wang, G.; Liu, L.; Wu, R.; Wu, Y.; Fang, C.; Zhou, X.; Jiao, J.; Gu, Y.; Zhou, H.; Xie, Z.; Sun, Z.; Chen, D.; Dai, K.; Wang, D.; Tang, W.; Yang, T. T. C. Study of the interactions of a novel monoclonal antibody, mAb059c, with the hPD-1 receptor. *Sci. Rep.* **2019**, *9*, 17830.
(55) Zhang, F.; Qi, X.; Wang, X.; Wei, D.; Wu, J.; Feng, L.; Cai, H.; Wang, Y.; Zeng, N.; Xu, T.; Zhou, A.; Zheng, Y. Structural basis of the therapeutic anti-PD-L1 antibody atezolizumab. *Oncotarget* **2017**, *8*, 90215.
(56) Wang, M.; Wang, J.; Wang, R.; Jiao, S.; Wang, S.; Zhang, J.; Zhang, M. Identification of a monoclonal antibody that targets PD-1 in a manner requiring PD-1 Asn58 glycosylation. *Commun. Biol.* **2019**, *2*, 392.
(57) Anderson, J. M.; Kier, B. L.; Jurban, B.; Byrne, A.; Shu, I.; Eidenschink, L. A.; Shcherbakov, A. A.; Hudson, M.; Fesinmeyer, R. M.; Andersen, N. H. Aryl-aryl interactions in designed peptide folds: Spectroscopic characteristics and optimal placement for structure stabilization. *Biopolymers* **2016**, *105*, 337−356.
(58) Greenfield, N. J. Using circular dichroism collected as a function of temperature to determine the thermodynamics of protein unfolding and binding interactions. *Nat. Protoc.* **2006**, *1*, 2527.
(59) Surface areas calculated using Dr.sasa for the entire CDR-H3 model hairpins excised from the corresponding X-ray crystal structures: Ribeiro, J.; Ríos-Vera, C.; Melo, F.; Schüller, A. Calculation of accurate interatomic contact surface areas for the quantitative analysis of non-bonded molecular interactions. *Bioinformatics* **2019**, *35*, 3499.
(60) Bockus, A. T.; Schwochert, J. A.; Pye, C. R.; Townsend, C. E.; Sok, V.; Bednarek, M. A.; Lokey, R. S. Going Out on a Limb: Delineating The Effects of β-Branching, N-Methylation, and Side Chain Size on the Passive Permeability, Solubility, and Flexibility of Sanguinamide A Analogues. *J. Med. Chem.* **2015**, *58*, 7409.
(61) Camenisch, G.; Alsenz, J.; van de Waterbeemd, H.; Folkers, G. Estimation of permeability by passive diffusion through Caco-2 cell monolayers using the drugs' lipophilicity and molecular weight. *Eur. J. Pharm. Sci.* **1998**, *6*, 313.
(62) Velický, M.; Bradley, D. F.; Tam, K. Y.; Dryfe, R. A. W. In Situ Artificial Membrane Permeation Assay under Hydrodynamic Control: Permeability-pH Profiles of Warfarin and Verapamil. *Pharm. Res.* **2010**, *27*, 1644.
(63) Naylor, M. R.; Ly, A. M.; Handford, M. J.; Ramos, D. P.; Pye, C. R.; Furukawa, A.; Klein, V. G.; Noland, R. P.; Edmondson, Q.; Turmon, A. C.; Hewitt, W. M.; Schwochert, J.; Townsend, C. E.; Kelly, C. N.; Blanco, M.-J.; Lokey, R. S. Lipophilic Permeability Efficiency Reconciles the Opposing Roles of Lipophilicity in Membrane Permeability and Aqueous Solubility. *J. Med. Chem.* **2018**, *61*, 11169.
(64) Matsson, P.; Doak, B. C.; Over, B.; Kihlberg, J. Cell permeability beyond the rule of 5. *Adv. Drug Delivery Rev.* **2016**, *101*, 42.
(65) Danelius, E.; Poongavanam, V.; Peintner, S.; Wieske, L. H. E.; Erdélyi, M.; Kihlberg, J. Solution Conformations Explain the Chameleonic Behaviour of Macrocyclic Drugs. *Chem.—Eur. J.* **2020**, *26*, 5231.
(66) Fouché, M.; Schäfer, M.; Berghausen, J.; Desrayaud, S.; Blatter, M.; Piéchon, P.; Dix, I.; Martin Garcia, A.; Roth, H.-J. Design and Development of a Cyclic Decapeptide Scaffold with Suitable Properties for Bioavailability and Oral Exposure. *ChemMedChem* **2016**, *11*, 1048.
(67) Zamora-Carreras, H.; Maestro, B.; Strandberg, E.; Ulrich, A. S.; Sanz, J. M.; Jiménez, M. Á. Micelle-Triggered β-Hairpin to α-Helix Transition in a 14-Residue Peptide from a Choline-Binding Repeat of the Pneumococcal Autolysin LytA. *Chem.—Eur. J.* **2015**, *21*, 8076.
(68) Nielsen, D. S.; Lohman, R.-J.; Hoang, H. N.; Hill, T. A.; Jones, A.; Lucke, A. J.; Fairlie, D. P. Flexibility versus Rigidity for Orally Bioavailable Cyclic Hexapeptides. *ChemBioChem* **2015**, *16*, 2289.
(69) Yamashita, H.; Kato, T.; Oba, M.; Misawa, T.; Hattori, T.; Ohoka, N.; Tanaka, M.; Naito, M.; Kurihara, M.; Demizu, Y. Development of a Cell-penetrating Peptide that Exhibits Responsive Changes in its Secondary Structure in the Cellular Environment. *Sci. Rep.* **2016**, *6*, 33003.
(70) Heimark, L. D.; Trager, W. F. The preferred solution conformation of warfarin at the active site of cytochrome P-450 based on the CD spectra in octanol/water model system. *J. Med. Chem.* **1984**, *27*, 1092.
(71) Cândido, E. S.; Cardoso, M. H.; Chan, L. Y.; Torres, M. D. T.; Oshiro, K. G. N.; Porto, W. F.; Ribeiro, S. M.; Haney, E. F.; Hancock, R. E. W.; Lu, T. K.; de la Fuente-Nunez, C.; Craik, D. J.; Franco, O. L. Short Cationic Peptide Derived from Archaea with Dual Antibacterial Properties and Anti-Infective Potential. *ACS Infect. Dis.* **2019**, *5*, 1081.
(72) Shimizu, K.; Mijiddorj, B.; Usami, M.; Mizoguchi, I.; Yoshida, S.; Akayama, S.; Hamada, Y.; Ohyama, A.; Usui, K.; Kawamura, I.; Kawano, R. De novo design of a nanopore for single-molecule detection that incorporates a β-hairpin peptide. *Nat. Nanotechnol.* **2022**, *17*, 67.
(73) Richards, D. A. Exploring alternative antibody scaffolds: Antibody fragments and antibody mimics for targeted drug delivery. *Drug Discovery Today Technol.* **2018**, *30*, 35.

https://doi.org/10.1021/acsmedchemlett.2c00486
ACS Med. Chem. Lett. 2023, 14, 278−284